Geology, Geophysics & Environment 2024, vol. 50 (1): 77–92

Multi-stage fault formation and REE distribution in the surrounding Devonian dolomites in the south-eastern part of the Holy Cross Mountains (Poland)

Marek Nieć[1], Maciej Pawlikowski[2], Edyta Sermet[3]

[1] *Mineral and Energy Economy Research Institute of the Polish Academy of Sciences, Krakow, Poland, e-mail: niecm@wp.pl, ORCID ID: 0000-0001-6689-034X*
[2] *AGH University of Krakow, Faculty of Geology, Geophysics and Environmental Protection, Department of Mineralogy, Petrography and Geochemistry, Krakow, Poland, e-mail: mpawlik@agh.edu.pl, ORCID ID: 0000-0001-8604-7552*
[3] *AGH University of Krakow, Faculty of Geology, Geophysics and Environmental Protection, Department of Geology of Mineral Deposits and Mining Geology, Krakow, Poland, e-mail: sermet@agh.edu.pl (corresponding author), ORCID ID: 0000-0002-0360-9642*

Received: 23 May 2023; accepted: 20 December 2023; first published online: 16 February 2024

Abstract: Metallogenic studies carried out in the Holy Cross Mountains indicate a relationship between mineralization and fault tectonics in Devonian formations. The impact of fault formation on the geochemistry of host rocks has not yet been studied. Mineralogical and geochemical studies of fault core gouges and damage zones in the fault walls of Devonian dolomites in the Budy and Jurkowice quarries were carried out. In the clay-carbonate filling of the fault fissure, the presence of two generations of Fe sulfides, the increased content of Zr, Nb, U and Th in relation to the surrounding rocks was noted. In the fault walls of the dolomites, iron sulfide and hematite mineralization were found. Research on the REE content indicates that it is lower in the fault walls than in those located far from it, while it is clearly higher in the fault gouge, especially in terms of the content of "heavy" elements (HREE). This indicates both the supply of some components to the fault zone from external sources and their displacement from the surrounding rocks. It was also found that the fault was renewed before and after the Neogene at least twice (Badenian).

Keywords: Holy Cross Mountains, Devonian dolomites, fault zone, mineralization, rare earths

INTRODUCTION

Fault zones are ways in which fluids migrate in the rock massif and are of special interest in ore deposit geology, primarily as sites of mineralization, together with their surroundings which have a halo of elements dispersed around these deposits. The processes of mineral substance displacement and hydrothermal transformations in the vicinity of faults, caused by the movement of fluids in a variable tectonic stress field, were also studied (Jaroszewski 1986, Bruhn et al. 1994, Jébrak 1997, Gratier et al. 2013). Fault zones are also of interest as routes for fluid migration in the earth's crust and as indicators of seismicity (Delle Piane et al. 2017). The processes taking place in large regional fault zones activated by earthquakes is of particular interest (Ishikawa et al. 2014 and literature cited therein).

The example of a fault presented below brings interesting observations on the behavior of selected chemical elements within the fault core and in the surrounding carbonate rocks. It also allows us

to trace the history of the fault's development as one of the many recorded in the area of the Paleozoic massif of the Holy Cross Mountains.

A characteristic feature of this massif is the occurrence of numerous regional transversal faults, with a displacement of up to several hundred meters (Mizerski & Orłowski 1992), as well as sublatitudinal dislocations with a distinct horizontal shift component (Konon 2007, 2015). They were formed in the Late Carboniferous after the main folding of Variscan movements (Mizerski 1998, 2007), in the Mississippian and Early Permian (Wójcik et al. 2012). Their Caledonian foundations as well as later, the Maastrichtian-Palaeocene (Laramide) or younger reactivation are also a matter of debate (Kutek & Głazek 1972, Lamarche et al. 1999, Mizerski 2007). Numerous manifestations of ore and ore-free mineralization are associated with these fault zones (Rubinowski et al. 1966). Rubinowski (1971) distinguished two metallogenic epochs: Variscan and post-Variscan. During the Variscan epoch epigenetic iron and copper sulfide mineralization in the company of Co, Ni and Zn was formed. The post-Variscan is the epigenetic galena-barite mineralization, considered to be related to the Laramide phase of tectonic movements. This raises the question of the impact of the post-Variscan tectonics on Variscan mineralization.

The subject of the present study are the two submeridional faults registered in Middle Devonian dolomites from the Budy and Jurkowice quarries located in the Jurkowice element of the south-eastern part of the Kielce Region of the Holy Cross Mountains (Jurkowice Block). Attention was paid to the diversification of the content of trace elements in the fault zone, especially REE. The two-fold renewal of the fault was also noticed.

THE JURKOWICE BLOCK

The Jurkowice Block ("element" acc. to Romanek 1977) is located in the south-eastern part of the Holy Cross Mountains on the southern wing of the Klimontów anticlinorium (Fig. 1). It is considered a fragment of a W–E tectonic trench filled by Middle Devonian dolomites bordered on northern limb by Lower Devonian clastic formations and subordinated Silurian (Romanek & Rup 1989). The general geology of the block was presented by Romanek (1977). More detailed data are provided by bore holes drilled during the exploration of dolomite deposits and from outcrops on the walls of the Budy and Jurkowice quarries (Fig. 1)

In Jurkowice Quarry, Eifelian dolomites of Wojciechowice and Barania Góra formations-Jurkowice member are present (Wójcik 2016).

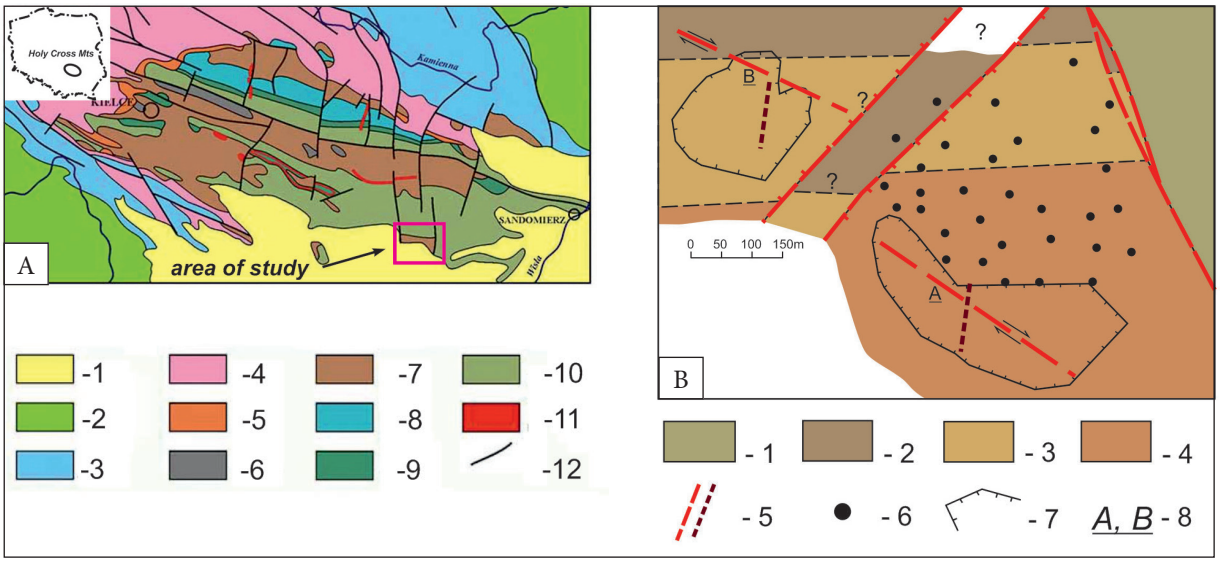

Fig. 1. *Location (A) (acc. to Salwa 2017, simplified): 1 – Neogene fms, 2 – Cretaceous fms, 3 – Jurassic fms, 4 – Triassic fms, 5 – Permian fms, 6 – Carboniferous fms, 7 – Devonian fms, 8 – Silurian fms, 9 – Ordovician fms, 10 – Cambrian fms, 11 – igneous rocks (lamprophyre and diabase), 12 – faults; general geology of the research area without Neogene cover (B): 1 – Cambrian, 2 – Lower Devonian, 3 – Middle Devonian Eifelian, 4 – Middle Devonian Givetian, 5 – faults, 6 – boreholes, 7 – contour of the quarry, 8 – studied faults*

In Budy Quarry, Middle Devonian – Givetian dolomitized limestones of the Kowala Formation occur (Narkiewicz 1987, 1991). They are locally covered with Neogene-Badenian deposits with varying degrees of thickness of up to a few meters, caused by their deposition on the rough top surface of Devonian rocks, often filling narrow deep depressions.

These are sands with a horizon of dolomite boulders with numerous traces of lithophaga (bivalves) activity, sandstones, mudstones with plant detritus, lithotamnium detrital limestone and local caliche like covers (Sermet et al. 2016).

The Jurkowice block is cut off from the east by the Samotnia dislocation (Romanek 1977) and dissected by numerous faults. The most prominent are NE–SW faults bordering a horst located between Jurkowice and Budy quarries and the NWW–SEE strike-slip fault zone that contains a breccia core up to a few meters thick and locally formed by slabs of folded wallrocks in the deformation zone. The brecciated dolomites and dolomites in the fault surroundings are irregularly recrystallized to varying degrees, replaced by illite and partly silicified, impregnated by finely dispersed hematite or iron sulfides (Nieć & Pawlikowski 2015).

The submeridional N–S to NNE–SSW dissect the whole suite of dolomitic rocks exposed in the Budy and Jurkowice quarries and are the object of a detailed study presented below.

THE STUDIED FAULTS AND THEIR SURROUNDINGS

In the Budy Quarry, the normal NNE–SSW trending fault with at least 10-metres thrust was exposed on six quarry levels, e.g. about 50 m in vertical section (Figs. 2, 3). It is also clearly marked below on the electrical resistivity tomography section as a zone of very low resistance associated with the presence of iron sulfide mineralization (Fig. 4).

In the area of the fault occurrence, the Devonian dolomites were covered by sandy Neogene-Badenian mudstones with plant detritus, over which sandy lithotamnian limestones and caliche, partly silicified cover. Recently it is removed by exploitation. The age of the fault is undetermined. It can be associated with the system of Late Variscan dislocations cutting through the Paleozoic massif of the Holy Cross Mountains, but its later renewal can also be demonstrated.

Fig. 2. *The studied fault in the Budy Quarry*

Fig. 3. *NNE–SSW fault in the Budy Quarry at III, IV and V exploitation level: 1–5 – sample location (see Table 1)*

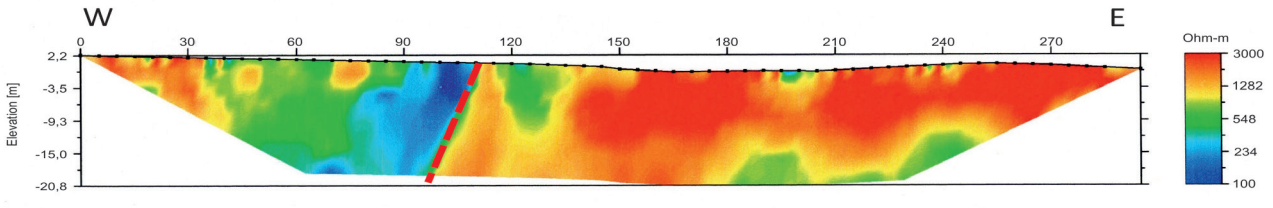

Fig. 4. *Fault zone on electrical resistivity tomography section below the quarry footwall (Gawron 2010)*

The Dolomites crossed by the fault are gray in color due to the presence of a small amount of finely dispersed FeS_2. Its oxidation means they become light brown as a result of weathering at the highest levels of the mine, to about 20–30 m in depth, with the presence of overlying Neogene formations suggesting pre-Neogene weathering. The presence of such weathered dolomites in only one flank of the fault (Fig. 2) also suggests its renewal before the Neogene with about 10 m displacement. In the overlying silicified lithotamnia Neogene limestones, a small fault with about 1 m thrust could be observed, thus some renewal of the fault also occurred after the Badenian.

The fault fissure, from a few to several centimeters wide, is filled with a black clay gouge, with rare, finely crushed fragments of dolomite (Fig. 5). In the fault walls, within the damage zone in the Devonian dolomites, small feather faults and joints appear, accompanied by crackle, mosaic breccia, and veins of coarse-crystalline dolomite.

The dolomites in the fault walls are locally mineralized with iron sulfides (marcasite-pyrite), which are replaced by hematite at a distance of several centimeters to several meters from the fault core.

Sulfide mineralization occurs irregularly, usually in the form of impregnation and discontinuous coatings on the crack walls (Fig. 6) or the filling of thick cracks up to 1–2 mm, less often in the form of discontinuous, irregular veins with a thickness of several centimeters and in nest clusters. The FeS_2 content in samples with of 1–2 dm^3 volume can then reach some dozen percent. It also appears as cementing breccia, in the company of coarse-crystalline dolomite. Then it forms irregular coatings on the brecciated rock fragments The crystalline dolomite fills the remaining space or sometimes separates the sulfide bands from the breccia fragments (Fig. 7C). Iron sulfide aggregates are also brecciated and cemented by the generation of younger crystalline dolomites (Fig. 7A, B).

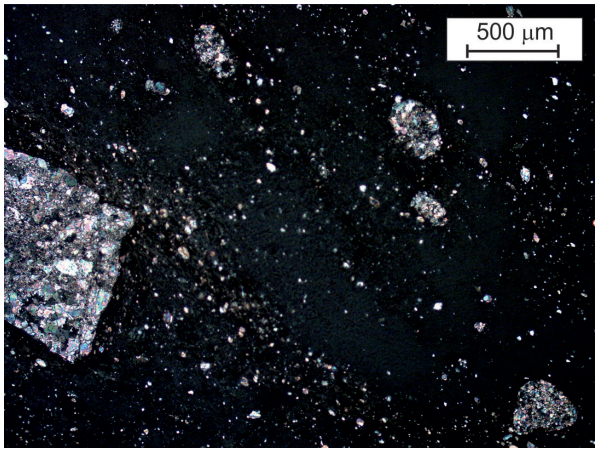

Fig. 5. *Fine dolomite fragments in the fault gouge (transmitted polarized light)*

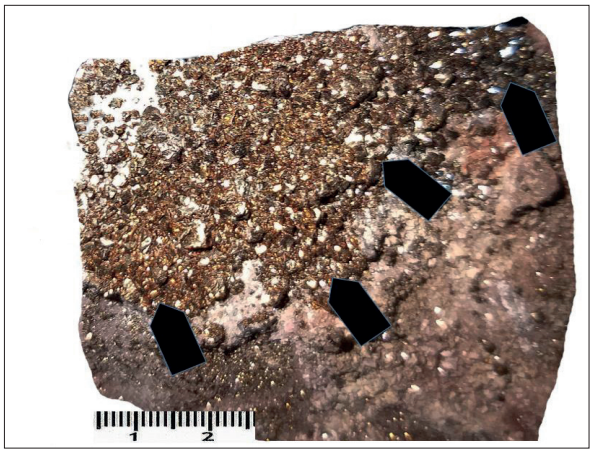

Fig. 6. *Iron sulfide crust (black arrows) on the fracture plane*

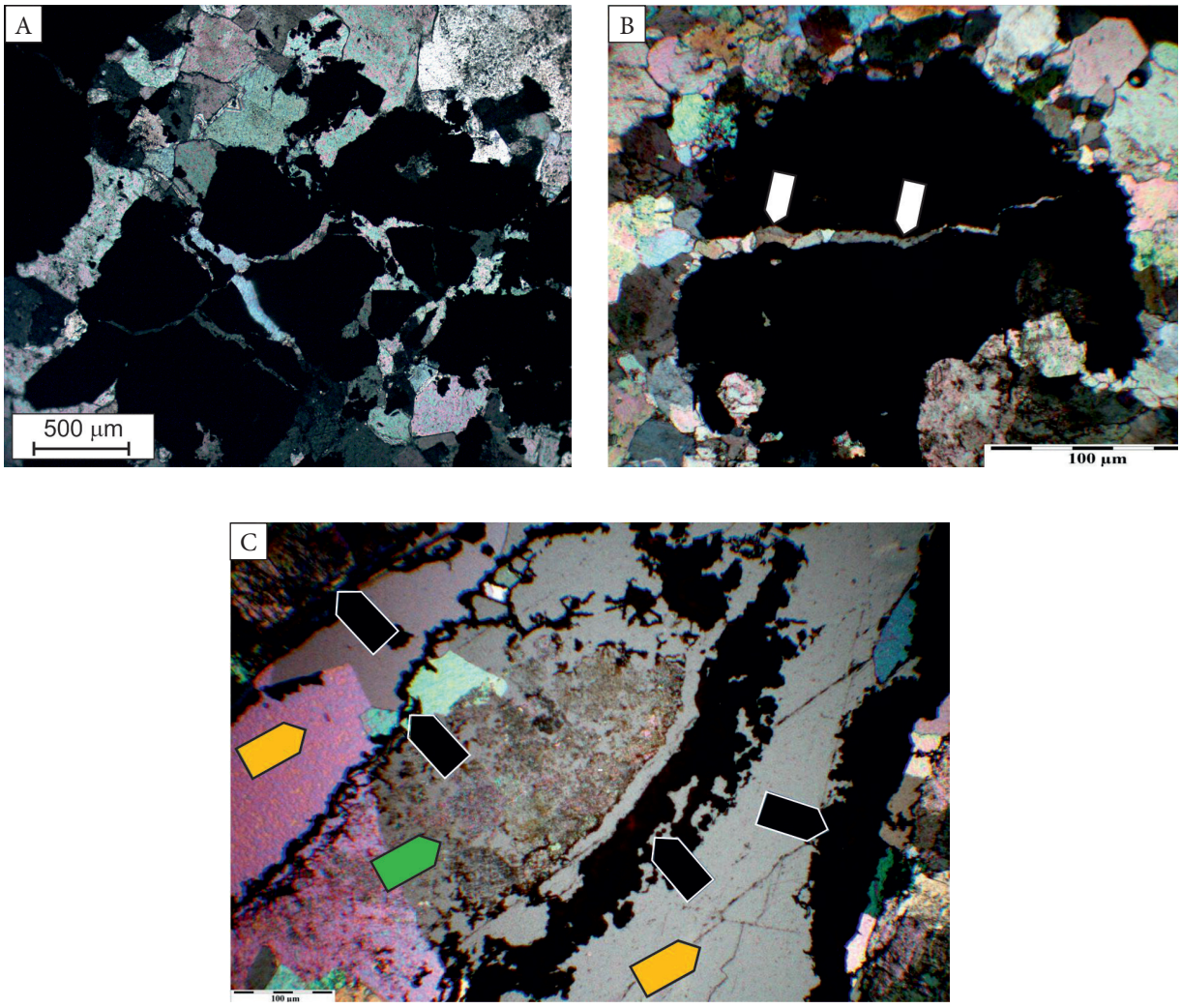

Fig. 7. *Brecciated marcasite-pyrite aggregates (A), broken iron sulfide aggregate (B), and brecciated dolomite rock fragment (green arrow) surrounded by iron sulfides (black arrows) and crystalline dolomite (yellow arrows) (C); transmitted polarized light*

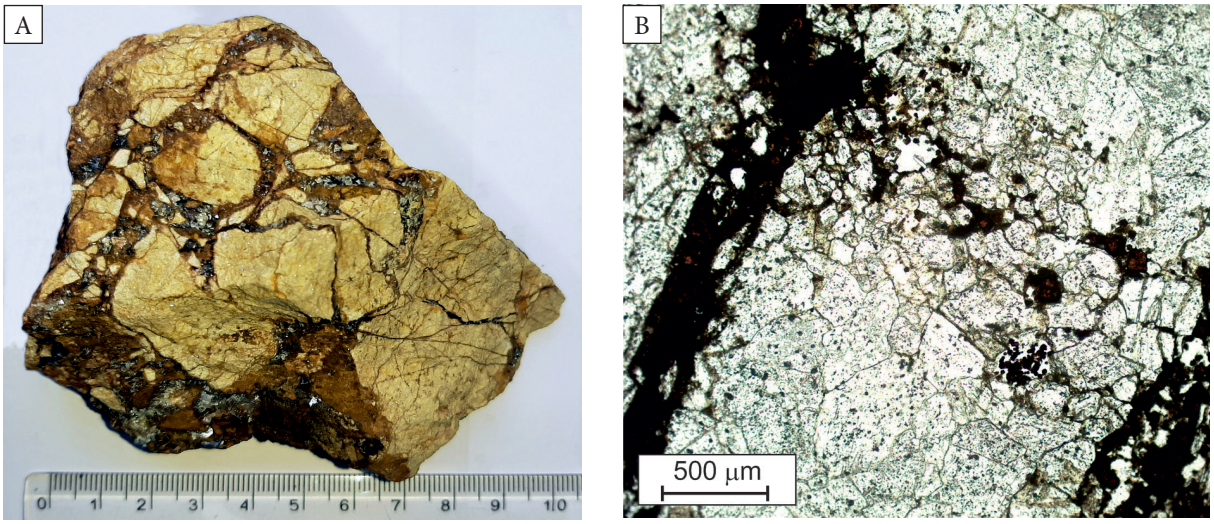

Fig. 8. *Mineralization in the weathering zone: A) hydrated iron oxides with calcite in the dedolomite breccia cement; B) hydrohematite-goethite veins and impregnations (transmitted polarized light)*

In the weathering zone, sulfides are completely replaced to a depth of approx. 10–20 m from the surface by hydrated iron oxides, which form a network of veins, and dolomite breccia cement (Fig. 8). The host rock in this zone is affected by dedolomitization, and calcite appears inside the veins of hydrated Fe oxides.

METHODS

The "fault gouge", mineralized dolomites in the fault walls, and unmineralized dolomites at a distance of several meters from the fault zone were sampled on several levels of the mine following exploitation advancement. Due to the requirements of mining supervision regarding the safety rules, samples could only be taken in certain places, and therefore in a random manner.

Field macroscopic observations were supported by binocular magnifying glasses and thin and polished section studies in polarized light. A FEI Quanta 200 FEG scanning microscope was used for detailed studies of the fault gouge. Chemical analyses in the micro-area were performed using an EDS detector carried out in the "low vacuum" mode. The research of the thicker fraction separated from the fault gouge was carried out in the Trace Elements Laboratory of the AGH-KGHM using a Jeol Super Probe 8230 electron microprobe equipped with a number of spectrometers for chemical analyses. X-ray diffraction tests were performed with a DRON 2.5 diffractometer and monochromatic Cu Kα radiation used. For the interpretation of the results, the XRAYAN computer identification program was used.

Chemical analyses were performed in the AcmeLabs laboratory (Bureau Veritas), with samples weighing approx. 1 kg being crushed into approx. 2 mm grains. After mixing, they were reduced in a Jones splitter to 250 µm, before being ground to 75 µm size.

The analytical 0.5 g sample after lithium borate fusion was dissolved in aqua regia. ICP-ES/MS analyses were performed according to the standard LF 200 and A 200 AcmeLabs procedure.

RESULTS

Clay minerals are the main components of the fault gouge, with 3% content of iron sulfides and the significantly higher content of TiO_2, Zr, Hf, Nb, Th, U compared to the surrounding dolomites and, less clearly, V, Co, Ni, As, Zn, Pb, Mo (Table 1, Figs. 9, 10). The dolomites, FeS_2 mineralized in the vicinity of the fault are characterized by increased contents of Zn, Pb, Co, Ni, As. Mo which can be associated with the presence of iron sulfides.

Table 1
Analyzed samples taken at the IV exploitation level

Recorded components	Fault gouge	Dolomites mineralized in the fault walls		Dolomites distant from the fault	
		with FeS_2	with Fe_2O_3		
	1	2	3	4	5
[%]					
SiO_2	32.69	2.91	0.87	5.49	7.19
Al_2O_3	18.49	1.53	0.41	1.29	2.58
Fe_2O_3	3.23	9.66	0.82	0.63	1.19
MgO	9.15	16.17	20.24	19.44	18.40
CaO	8.90	24.11	30.63	28.77	26.59
Na_2O	0.15	0.02	0.03	0.03	0.04
K_2O	3.37	0.36	0.11	0.36	0.73
S	1.35	7.49	0.07	0.07	0.26
TiO_2	0.92	0.06	0.02	0.06	0.13
[ppm]					
Zr	309.3	15.7	4.8	12.4	33.3
Hf	7.8	0.4	0.1	0.3	0.6
Nb	20.2	0.9	<0.1	0.7	2.6
Th	14.3	0.9	0.3	0.9	1.9
U	12.1	2.5	1.1	1.4	2.9
V	98	47	<8	13	21
Co	6.5	5.6	2.2	1.3	1.8
Ni	26.4	14.0	5.5	4.9	6.5
As	27.4	21.0	1.5	1.6	4.3
Cu	3.5	4.2	2.0	1.9	1.5
Pb	8.0	24.9	0.9	1.4	2.2
Zn	69	65	12	8	15
Mo	1.0	1.3	0.3	0.1	0.2
La	6.7	4.8	4.8	6.3	6.3
Ce	12.3	9.3	8.7	13.1	13.2
Pr	1.50	1.11	0.94	1.44	1.47
Nd	6.1	4.2	3.6	5.3	5.8
Sm	1.28	0.77	0.54	0.97	1.09
Eu	0.25	0.13	0.10	0.22	0.20
Gd	1.25	0.69	0.51	1.01	1.09
Tb	0.21	0.10	0.07	0.16	0.15
Dy	1.32	0.63	0.43	0.98	0.85
Ho	0.30	0.13	0.09	0.19	0.20
Er	1.02	0.34	0.26	0.60	0.52
Tm	0.16	0.05	0.03	0.08	0.10
Yb	1.21	0.31	0.20	0.49	0.61
Lu	0.20	0.03	0.03	0.07	0.07
Y	8.5	3.6	2.8	5.2	4.7

1 – clayey fault gouge, 2 – mineralized dolomites in the fault walls, 3 – not mineralized dolomites in the fault walls, 4, 5 – dolomite located far from the fault zone.

The unmineralized dolomites in the fault vicinity do not differ from those located further away, although the variation in the content of rare earth elements is interesting (Figs. 11, 12). This reaches 40–41 ppm in the dolomites outside the fault zone, 434 ppm in the fault clay gouge, while it is clearly lower in the fault walls damage zone and amounts to 26–28 ppm. The variation of HREE content particularly marked: their enrichment in the fault gouge and depletion in dolomites in the fault walls in the damage zone. This suggests the REE displacement from the fault walls into the fault gouge.

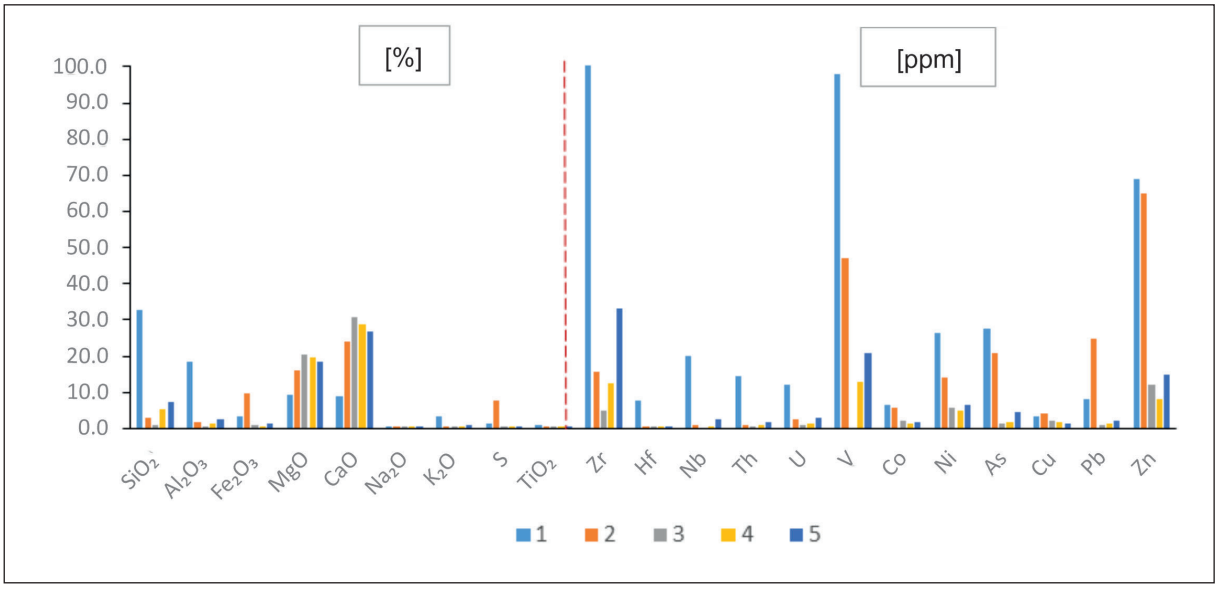

Fig. 9. *The content of selected components of the tested samples (% and ppm, respectively): 1 – fault gouge, 2 – mineralized dolomites in the fault walls, 3 – not mineralized dolomites in the fault walls, 4, 5 – dolomite located far from the fault zone*

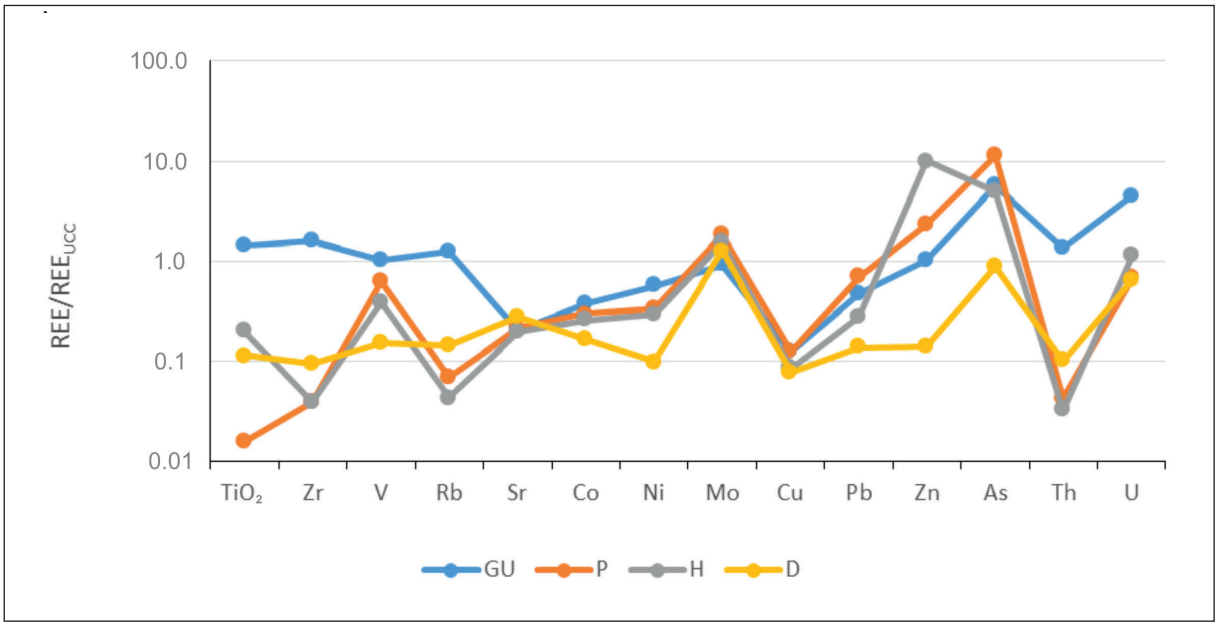

Fig. 10. *Average content of selected elements normalized to their content in the upper earth's crust (UCC acc. Rudnick & Gao 2014): GU – fault gouge, P, H – mineralized dolomites in the fault walls damage zone (P – iron sulfides, H – hematite), D – dolomites far from the fault zone*

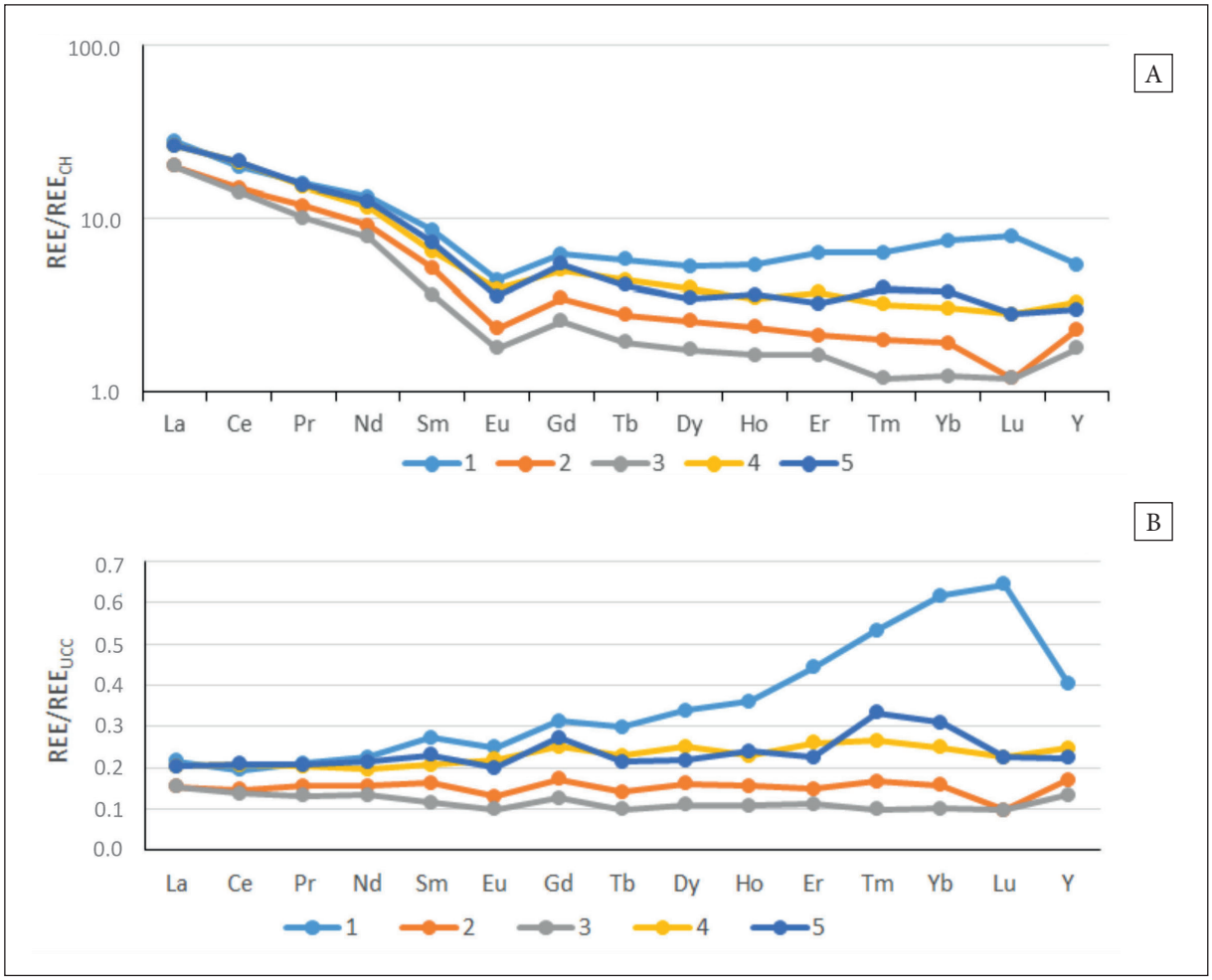

Fig. 11. *REE content normalized to chondrite (A) and upper crust (B) in samples from IV exploitation level: 1 – fault gouge, 2 – mineralized dolomites in the fault walls, 3 – not mineralized dolomites in the fault walls, 4, 5 – dolomite located far from the fault zone*

Microscopic identification of the fault gouge forming minerals is practically impossible due to the presence of black and very poorly transparent material. Therefore, this material was screened into fractions <0.06 mm and 0.2–0.06 mm, and tested separately. The <0.06 mm grain size fraction was examined by phase X-ray diffraction, and the presence of dolomite, illite, calcite, kaolinite, titanite, pyrite and gypsum was identified. The elevated diffraction background pattern in the 20–40° 2Θ section (Fig. 13) proves the presence of a substance with a disordered atomic structure, i.e. heavy hydrocarbons (Fig. 13). The 0.2–0.06 m fraction (Fig. 14) was analyzed using a binocular loupe at magnifications up to 150× and microscopically in the polarized transmitted light.

Planimetric analysis performed under a binocular magnifying glass allowed us to identify dolomite as the main constituent of this fraction as well as ore minerals (Table 2, Figs. 14, 15). The CaO content varied from 57.43 to 59.83%, and MgO from 35.87 to 42.57% suggests that there are fragments of rocks unevenly dolomitized or dedolomitized as a result of weathering, indicated by the presence of gypsum. There are only few percent of ore minerals in this fraction, with the presence of galena, sphalerite and undetermined Mn minerals detected by electron microprobe analysis (Tables 2, 3, Fig. 16). Iron sulfides form two types of grains: finely crushed and microglobular aggregates (Fig. 17), suggesting two different sources.

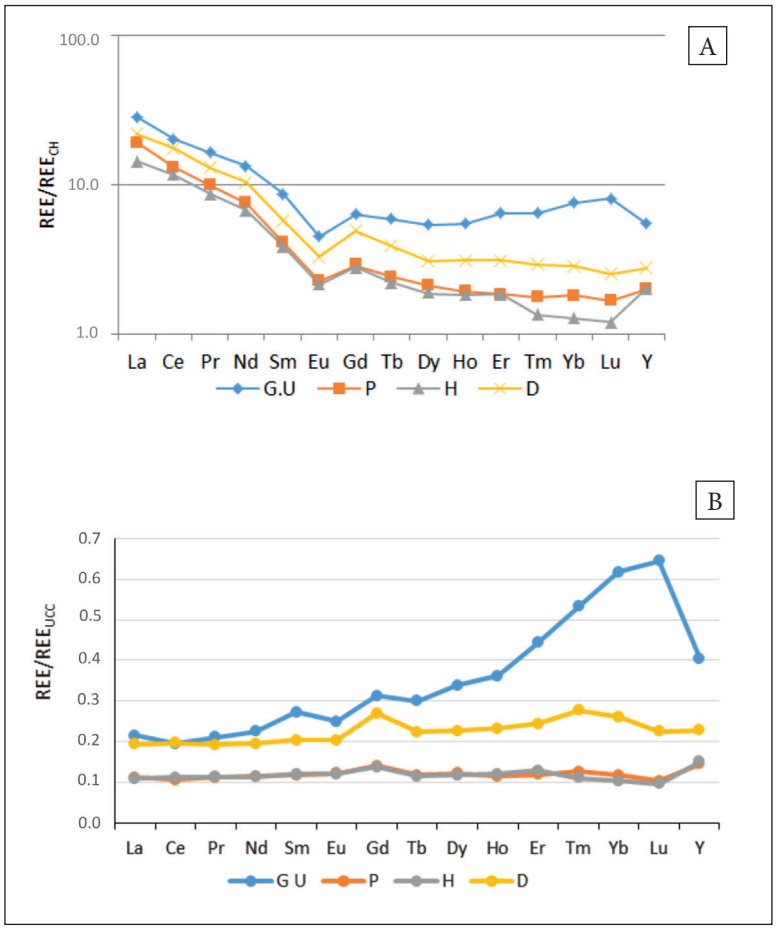

Fig. 12. *Mean REE content in samples taken at different quarry levels, normalized to chondrite (A) and upper crust (B): GU – fault gouge, P – dolomites FeS_2 mineralized (5 analyses), H – dolomites with hematite (3 analyses), D – barren dolomites (4 analyses)*

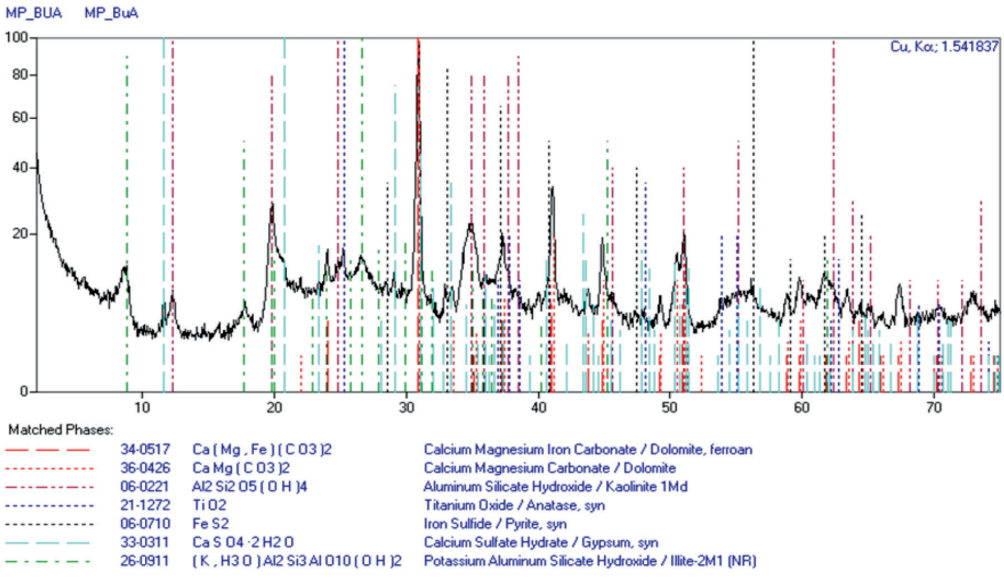

Fig. 13. *X-ray diffractogram of fine fraction <0.06 mm of fault gouge*

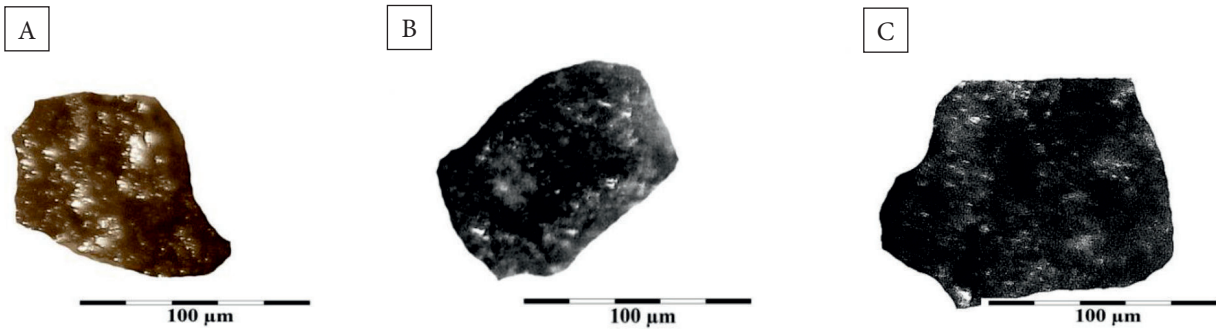

Fig. 14. *Ore mineral grains from the fault gouge: A) iron sulfide; B) galena; C) sphalerite*

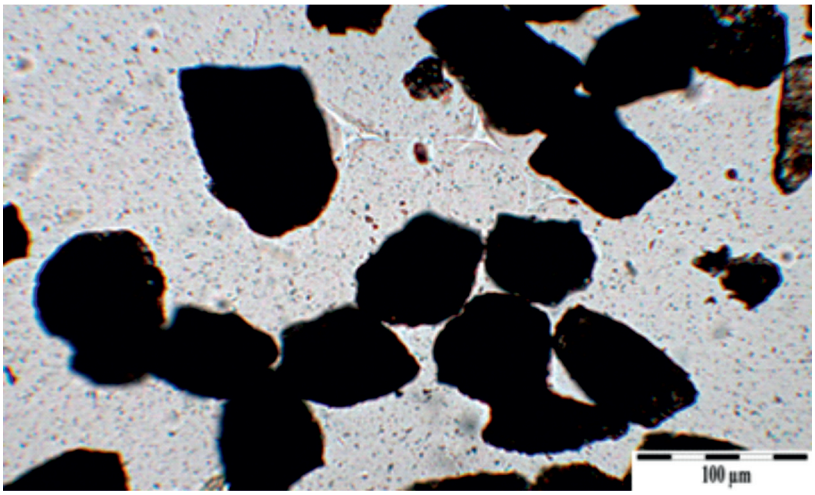

Fig. 15. *The electron microprobe studied ore mineral grains selected from the fault gouge*

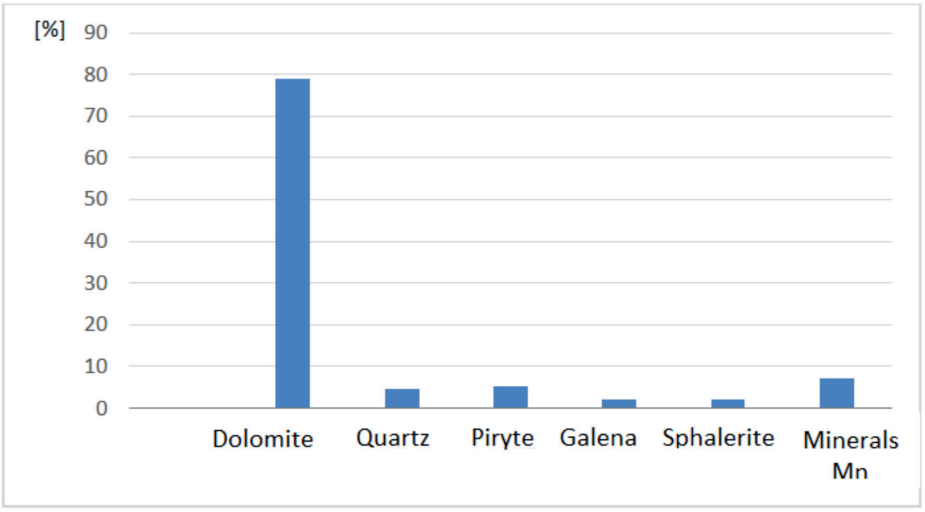

Fig. 16. *Mineral composition of <0.2 mm fraction*

Table 2
Results of planimetric analysis of material screened from fault clayey gouge

Mineral	Content [%]
Dolomite	79.0
Quartz	4.6
Piryte	5.3
Galena	2.1
Sphalerite	1.9
Minerals Mn	7.1

Crushed sulfide grains clearly indicate the brecciation of mineralized formations before the currently observed fault filling. This can be associated with the renewal of the fault, which also results in the brecciation of iron sulfide clusters present in the fault walls.

The high content of sulfur in relation to Fe in the iron sulfide grains identified as "pyrite" is noteworthy. The S/Fe % ratio is about 2, while in pyrite or marcasite it should be 1.17 (Fe 46%, S 54%). This suggests that the analyzed grains are enriched in sulfur towards Fe_3S_8 polysulfide.

Table 3
Results of electron microprobe chemical analyzes of Fe sulfides from fault gouge

Fe sulfide	S	Co	Fe	Ni	Zn	Sb	Cu	As	Total
	[wt.%]								
Microglobular	66.9681	0.0348	32.9777	0.0073	0.0022	0.0000	0.0099	0.0000	100.00
Angular (crushed)	66.9213	0.0284	33.0375	0.0000	0.0113	0.0000	0.0016	0.0000	100.00
	66.9236	0.0402	33.0210	0.0000	0.0118	0.0034	0.0000	0.0000	100.00
	66.7286	0.0389	33.2187	0.0129	0.0010	0.0000	0.0000	0.0000	100.00
	67.2562	0.0134	32.7147	0.0082	0.0032	0.0000	0.0043	0.0000	100.00
	67.0391	0.0326	32.9143	0.0023	0.0118	0.0000	0.0000	0.0000	100.00

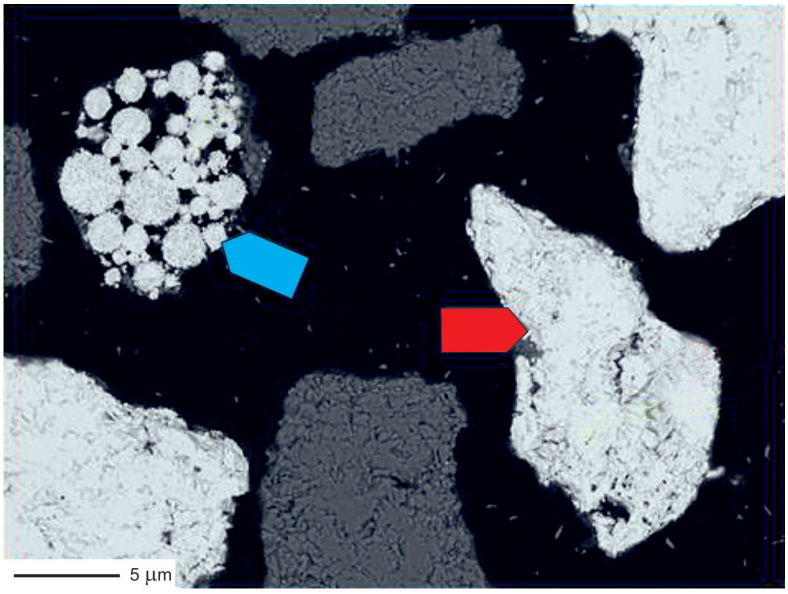

Fig. 17. *Two types of iron sulfide grains in the fault gouge. Microaggregate nodular pyrite (blue arrow) and crushed pyrite grains (red arrow). Electron microprobe*

The dolomites in the vicinity of the fault fissure are FeS_2 mineralized with varied intensity. The iron sulfide content varies within broad limits ranging from just a few percent to over a dozen, and exceptionally up to about 70% in locally occurring vein clusters. The increased but varied accompanying metal content is associated with this mineralization. Particularly remarkable is the predominance of Ni over Co (Fig. 18) and the increased content of vanadium. This suggests the regeneration of sulfides from older sedimentary formations.

The variation of the observed REE and other components in the vicinity of the fault suggests the presence of lateral secretion processes in their displacement.

A similar behavior of elements, in particular REE, was also found in the vicinity of a fault (Fig. 19) in the Eifelian dolomites in the Jurkowice Quarry.

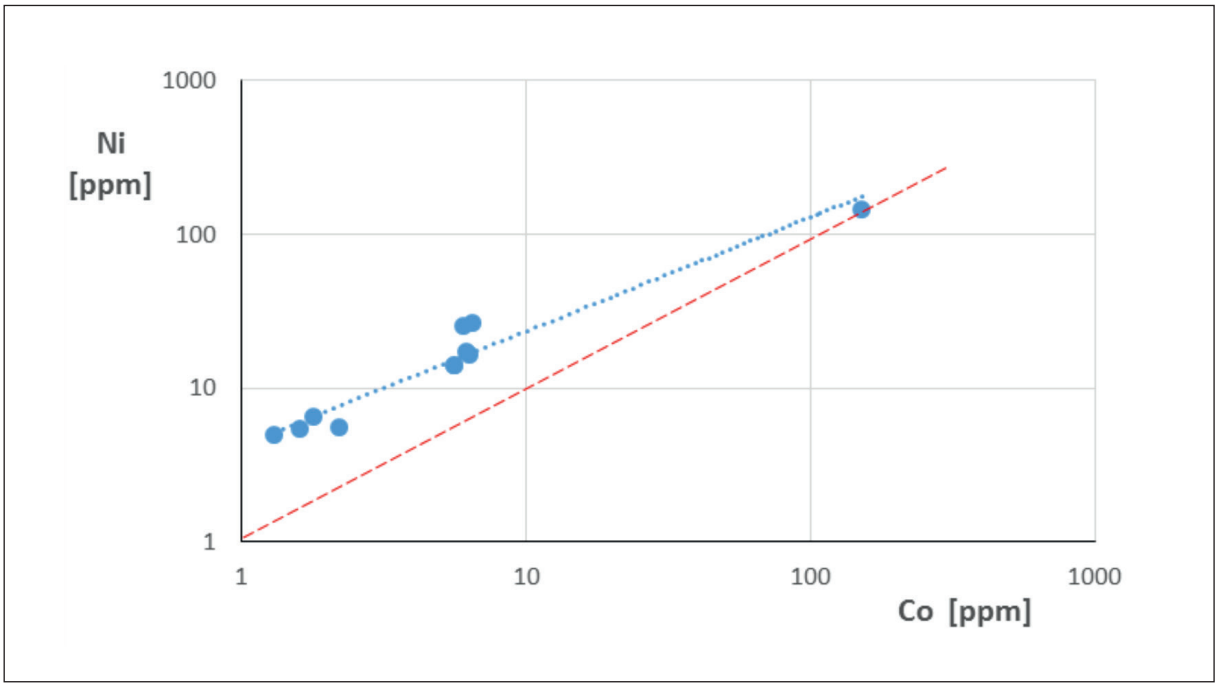

Fig. 18. *Co-Ni content relationship in samples with FeS_2.*

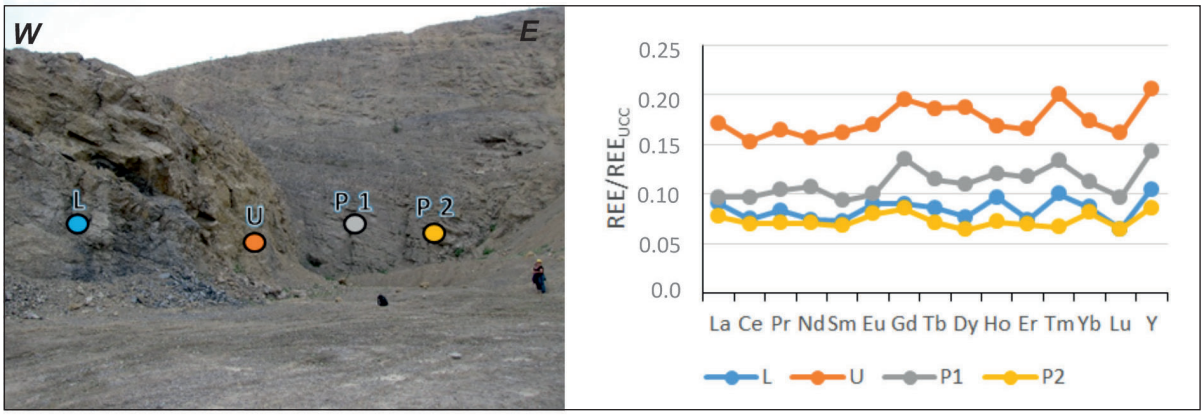

Fig. 19. *REE content in samples in the Jurkowice fault zone and its surroundings, normalized to the upper crust; U – brecciated dolomite in the fault zone, P, L – dolomites in the fault wings*

DISCUSSION

The studied faults are examples of the many which have been recorded in the Paleozoic Massif of the Holy Cross Mountains and which are generally of a similar orientation to the great transversal dislocations crossing this massif (Mizerski & Orłowski 1962). They were paths for the migration of mineralizing fluids which were rich in sulfur and contained chalcophile elements, although the low content of Cu is noteworthy. Also, interesting is the high content of Zr and Hf and increased levels of Ti, Nb, U and Th in relation to the surrounding undisturbed rocks. This suggests that they were supplied from an external source and concentrated in the clayey environment of the fault gouge.

Differences in the content of some elements in the fault gouge and surrounding dolomites, especially REE, can also be interpreted as stemming from their lateral movement and accumulation in the residual products of the removal of carbonate components in the fault fissure. However, a clear increase in the content of HREE in relation to LREE is noteworthy and suggests either the supply of HREE from the outside or the removal of LREE in the process. The general decrease in the total REE content in mineralized dolomites in relation to those occurring beyond the mineralization zone seems to indicate the supply of HREE to the fault core from beyond the immediate vicinity of the fault.

The mobility of LREE greater than HREE has often been reported in hydrothermal and weathering processes (Williams-Jones 2015, Migdisov et al. 2016), although the mobility of HREE is also reported (Yongliang & Yusheng 1991). The mobility of chemical components in fault zones is often found in the environment of aluminosilicate, igneous, and metamorphic rocks (Park & Kim 2014). It is also noted in the environment of carbonate rocks and associated with the movement of hydrothermal fluids. In addition to the supply of some elements from the outside, their lateral secretion movement to the fault core from wall rocks is also observed (Nuriel et al. 2011). A differentiation of REE content in fault zones is noted (Su et al. 2003), especially the enrichment of fault core (Liu et al. 2017) which is associated with their seismic activity (Manighetti et al. 2010, Mouslopoulou et al. 2011). An increase in the REE and Y content in their outcrops is also observed as a result of weathering processes.

In the considered fault case, sulfide-hematite mineralization indicates low-temperature hydrothermal processes (Nieć & Pawlikowski 2019), accompanied by the movement of LREE toward the fault core. Their enrichment in the fault gouge is enabled by the sorption properties of the clay minerals which are its main constituent.

CONCLUSIONS

The presence of fragmented iron sulfide aggregates in the fault clayey gouge indicates that its formation took place after the sulfide mineralization present in the dolomites in the fault walls. The presence of uncrushed sulfide clusters in it at the same time indicates a two-phase mineralization process separated by fault renewal.

The varied extent of the weathering zone in the fault walls and below the overlying Neogene formation presented above allow us to presume the fault renewal before the Neogene and the second phase of mineralization, or the regeneration of the older one. Lamarche et al. (1999) found the reactivation of meridional faults in the S–W part of the Holy Cross Mountains and associated it with tectonic processes in the Laramie phase during the Maastrichtian-Paleocene period. The above-presented observations of fault extension in the Neogene formations indicate at least two renewal phases of the examined fault i.e. before and after or during the Neogene, precisely before and after the Badenian.

The Jurkowice block is located on the border of the Paleozoic core of the Holy Cross Mountains and the Carpathian Foredeep, in the former coastal zone of the Neogene sea basin (Radwański 1973). In the Carpathian Foredeep, close to the studied area, tectonic movements are detected during and after the sedimentation of the Miocene formations (Pawłowski 1965, Radwański 1973, Romanek 1977). The renewal of older faults is a consequence of these movements and, in the case of the described fault, they occurred before and after the Lower Badenian.

The observed variation in REE content in the described fault zones suggest their local redistribution by mineralizing fluids. Fault related iron sulfide mineralization is analogous to that accompanying other Variscan faults (Nieć & Pawlikowski 2015). The contents of Ni and V in iron sulfides suggest that their primordial source could have been older sedimentary formations. Younger tectonic movements before and after the Lower Badenian caused the brecciation of sulfide aggregates and their partial regeneration. The rejuvenation of the Variscan mineralization has not been accounted for in former studies of the metallogeny of the Holy Cross Mountains.

The authors would like to thank the Presidents of PBI and the manager of the mine, Marek Zając M.Sc. Eng. for making it possible to conduct observations in the mine and helping in their field implementation. We also thank the reviewers for their valuable remarks.

This paper was implemented as part of research no. 16.16.140.315.

REFERENCES

Bruhn R.L., Parry W.T., Yonkee W.A. & Thompson T., 1994. Fracturing and hydrothermal alteration in normal fault zones. *Pure and Applied Geophysics – PAGEOPH*, 142(3/4), 609–644. https://doi.org/10.1007/BF00876057.

Delle Piane C., Clennell M.B., Keller J.V.A., Giwelli A. & Luzin V., 2017. Carbonate hosted fault rocks: A review of structural and microstructural characteristic with implications for seismicity in the upper crust. *Journal of Structural Geology*, 103, 17–36. https://doi.org/10.1016/j.jsg.2017.09.003.

Gawron P., Frycz M. & Długosz Ł., 2010. *Określenie stropu zalegania starszego podłoża wykształconego jako dolomity i wapienie dewońskie*. Archiwum Kopalń Dolomitu SA w Sandomierzu [unpublished].

Gratier J.P., Dysthe D.K. & Renard F., 2013. The role of pressure solution creep in the ductility of the Earth's upper crust. *Advances in Geophysics*, 54, 47–179. https://doi.org/10.1016/B978-0-12-380940-7.00002-0.

Ishikawa T., Hirono T., Matsuta N., Kawamoto K., Fujimoto K., Kameda J., Nishio Y., Maekawa Y. & Honda G., 2014. Geochemical and mineralogical characteristics of fault gouge in the Median Tectonic Line, Japan: evidence for earthquake slip. *Earth, Planets and Space*, 66(1), 36. https://doi.org/10.1186/1880-5981-66-36.

Jaroszewski W., 1986. Tektonika a mineralogeneza: wybrane aspekty [Tectonics versus mineralogenesis – selected aspects]. *Przegląd Geologiczny*, 34(10), 560–566.

Jébrak M., 1997. Hydrothermal breccias in vein-type ore deposits: A review of mechanisms, morphology and size distribution. *Ore Geology Review*, 12(3), 111–134. https://doi.org/10.1016/S0169-1368(97)00009-7.

Konon A., 2007. Strike-slip faulting in the Kielce unit, Holy Cross Mountains, central Poland. *Acta Geologica Polonica*, 57(4), 415–441.

Konon A., 2015. Tectonics of the Holy Cross Mountains folt belt. [in:] Sidorczuk M., Wańkiewicz A., Skompski S., Kozłowski W., Kozłowska M., Lindner L., Wysocka A., Olszewska-Nejbert D., Bąbel M., Głowniak E., Łuczyński P., Matyja B., Waksmundzki B., Leonowicz P., Górka M., Konon A., Radwański A., Barski M., Żylińska A. & Ziółkowski P., *The Holy Cross Mountains: 25 journeys through Earth history*, University of Warsaw, Faculty of Geology, Warszawa, 39–47.

Kutek J. & Głazek J., 1972. The Holy Cross area, Central Poland in the Alpine cycle. *Acta Geologica Polonica*, 22(4), 603–653.

Lamarche J., Mansy J.L., Bergerat F., Aveebuch O., Hakenberg M., Lewandowski M., Stupnicka E., Swidrowska J., Wajsprych W. & Wieczorek J., 1999. Variscan tectonics in the Holy Cross Mountains (Poland) and the role as structural inheritance during Alpine tectonics. *Tectonophysics*, 313(1–2), 171–186. https://doi.org/10.1016/S0040-1951(99)00195-X.

Liu Y., Wu K., Wang X., Pei Y., Liu B. & Guo J., 2017. Geochemical characteristics of fault core and damage zones of the Hong-Che fault zone of the Junggar Basin (NW China) with implications for the fault sealing process. *Journal of Asian Earth Sciences*, 143(1), 141–155. https://doi.org/10.1016/j.jseaes.2017.04.025.

Manighetti I., Boucher E., Chauvel C., Schlagenhauf A. & Benedett L., 2010. Rare earth elements record past earthquakes on exhumed limestone fault planes. *Terra Nova*, 22(6), 477–482. https://doi.org/10.1111/j.1365-3121.2010.00969.x.

Migdisov A., Williams-Jones A.E., Brugger J. & Caporuscio F.A., 2016. Hydrothermal transport, deposition and fractionation of the REE: Experimental data and thermodynamic calculations. *Chemical Geology*, 439, 13–42. https://doi.org/10.1016/j.chemgeo.2016.06.005.

Mizerski W., 1998. Podstawowe problemy tektoniki i tektogenezy utworów paleozoicznych Gór Świętokrzyskich [Main problems of tectonics and tectogenesis of the Paleozoic in the Holy Cross Mts (Central Poland)]. *Przegląd Geologiczny*, 46(4), 337–342.

Mizerski W., 2007. Holy Cross Mountains in the Caledonian, Variscan and Alpine cycles – major problems, open questions. *Przegląd Geologiczny*, 52(8/2), 774–779.

Mizerski W. & Orłowski S., 1992. Główne uskoki poprzeczne i ich znaczenie dla tektoniki antyklinorium klimontowskiego (Góry Świętokrzyskie). *Kwartalnik Geologiczny*, 37, 1, 19–40.

Mouslopoulou V., Moraetis D. & Fassoulas Ch., 2011. Identifying past earthquakes on carbonate faults: Advances and limitations of the 'Rare Earth Element' method based on analysis of the Spili Fault, Crete, Greece. *Earth and Planetary Science Letters*, 309(1–2), 45–55. https://doi.org/10.1016/j.epsl.2011.06.015.

Musiał A., Sermet E. & Nieć M., 2017. Rare Earth Elements in the rock sequence from Lower to Middle Devonian in the Holy Cross Mountains, Poland. [in:] *SGEM 2017: 17th International Multidisciplinary Scientific Geoconference: Science and Technologies in Geology, Exploration and Mining: 29 June–5 July, 2017, Albena, Bulgaria: Conference Proceedings. Vol. 17 iss. 11, Geology Mineral Processing*, STEF92 Technology Ltd., Sofia, 471–477.

Narkiewicz M., 1981. Budy – kamieniołom dolomitów i wapieni środkowego dewonu. [in:] Żakowa H. (red.), *Przewodnik LIII Zjazdu Polskiego Towarzystwa Geologicznego, Kielce, 6–8 września 1981: praca zbiorowa*, Wydawnictwa Geologiczne, Warszawa, 276–291.

Narkiewicz M., 1991. *Procesy dolomityzacji mezogenetycznej na przykładzie żywetu i franu Gór Świętokrzyskich*. Prace Państwowego Instytutu Geologicznego, 132, Wydawnictwa Geologiczne, Warszawa.

Nieć M. & Pawlikowski M., 2015. Mineralizacja markasytowo-hematytowo-ankerytowa w południowo wschodniej części Gór Świętokrzyskich. *Przegląd Geologiczny*, 69, 4, 219–227.

Nieć M. & Pawlikowski M., 2019. Dolomite-illitic rock (dollillite) – the product of hydrothermal replacement of carbonate rocks in the Holy Cross Mts. Poland – a possible guide to ores. *Geological Quarterly*, 63(2), 275–295. https://doi.org/10.7306/gq.1474.

Nuriel P., Rosenbaum G., Uysal T. I., Zhao J., Golding S. D., Weinberger R., Karabacak V. & Avani Y., 2011. Formation of fault related calcite precipitates and their implications for dating fault activity in the East Anatolian and Dead Sea fault zones. [in:] Fagereng Å. & Rowland J.V. (eds.), *Geology of the Earthquake Source: A Volume in Honour of Rick Sibson*, Geological Society, London, Special Publications, 359, Geological Society of London, 229–248. https://doi.org/10.1144/SP359.13.

Park S. & Kim Y., 2014. Mineralogy and geochemistry of Fault Gouge in pyrite-rich andesite. *Journal of Mineralogical Society of Korea*, 27(4), 301–310. https://doi.org/10.9727/jmsk.2014.27.4.301 [in Korean, with English abstract].

Pawłowski S., 1965. Zarys budowy geologicznej okolic Chmielnika – Tarnobrzega. [in:] Pawłowski S. (red.), *Przewodnik XXXVIII Zjazdu Polskiego Towarzystwa Geologicznego: Tarnobrzeg, 21–24 sierpnia 1965*, Wydawnictwa Geologiczne, Warszawa, 8–20.

Radwański A., 1973. Transgresja dolnego tortonu na południowo-wschodnich i wschodnich stokach Gór Świętokrzyskich. *Acta Geologica Polonica*, 23(2), 325–432.

Romanek A., 1977. *Objaśnienia do Szczegółowej mapy geologicznej Polski 1:50 000: arkusz Klimontów (887)*. Wydawnictwa Geologiczne, Warszawa.

Romanek A. & Rup M., 1989. Szarogłazy z Jurkowic na tle górnosylurskiej serii szarogłazowej południowej części Gór Świętokrzyskich. *Biuletyn Państwowego Instytutu Geologiczne*go, 362, 41–64.

Rubinowski Z., 1971. Rudy metali nieżelaznych w Górach Świętokrzyskich i ich pozycja metalogeniczna. *Biuletyn – Instytut Geologiczny*, 247, *Z Badań Złóż Kruszców w Polsce*, 8, 5–166.

Rubinowski Z., Kowalczewski Z., Lenartowicz L. & Wróblewski T., 1966. *Metalogeneza trzonu paleozoicznego Gór Świętokrzyskich*. Prace – Instytut Geologiczny, Wydawnictwo Geologiczne, Warszawa.

Rudnick R.L. & Gao S., 2014. Composition of the continental crust. [in:] Holland H.D. & Turekian K.K. (eds.), *Treatise on Geochemistry*, 3, Elsevier, Amsterdam, 1–64.

Salwa S., 2017. Mapa geologiczna Gór Świętokrzyskich. [in:] Nawrocki J. & Becker A. (red.), *Atlas geologiczny Polski*, Państwowy Instytut Geologiczny – Państwowy Instytut Badawczy, Warszawa, 32.

Sermet E., Musiał A. & Auguścik J., 2016. Geotopy południowo-wschodniej części Gór Świętokrzyskich [Geotourist attractions in the south-eastern part of the Holly Cross Mountains]. *Biuletyn Państwowego Instytutu Geologicznego*, 466, 271–277.

Su C., Li Y. & Wang Y., 2003. REE geochemistry as an indicator of activity of faults. [in:] *Proceedings of the International Symposium on Water Resources and the Urban Environment: 9–10 November 2003, Wuhan, P.R. China*, China Environmental Science Press, 565–570. https://www.researchgate.net/publication/288476877.

Williams-Jones A.E., 2015. The hydrothermal mobility of the rare earth elements. [in:] Simandl G.J. & Neetz M. (eds.), *Symposium on Strategic and Critical Materials Proceedings, November 13–14, 2015, Victoria, British Columbia*, British Columbia Geological Survey Paper, 2015-3, British Columbia Ministry of Energy and Mines, 119–123.

Wójcik E., Pelc A., Pacek A., 2012. Late Variscan deformation events in the Bardo Syncline revealed by biotite K-Ar dating of Ludlow-age tuffite (Holy Cross Mountains, Poland). *Geological Quarterly*, 65(1), 15. https//doi.org/10.7306/gq 1586.

Wójcik K., 2015. The uppermost Emsian and lower Eifelian in the Kielce Region of the Holy Cross Mts. Part I: Lithostratigraphy. *Acta Geologica Polonica*, 65(2), 141–179. https://doi.org/10.1515/agp-2015-0006.

Yongliang X. & Yusheng Z., 1991. The mobility of rare earth elements during hydrothermal activity: A review. *Chinese Journal of Geochemistry*, 10(4), 295–306. https://doi.org/10.1007/BF02841090.